

## f-electron Dualism as a Reason of Superconductivity in Ferromagnetic UGe<sub>2</sub>

Robert Troc\*

W. Trzebiatowski Institute of Low Temperature and Structure Research, Polish Academy of Sciences,  
P.O. Box 1410, 50-950 Wrocław 2, Poland

(Received 17 August 2004)

Magnetization and electrical resistivity measurements in the wide temperature and field ranges were performed on single crystals of UGe<sub>2</sub>. The presence of extremely large anisotropy in the temperature dependence of the susceptibility and magnetization has confirmed the previously published results. The dependence of spontaneous magnetization,  $\sigma_s$ , on temperature has been inferred from the Arrot plot and compared to that determined from neutron diffraction data. The earlier transversal and present longitudinal results on the magnetoresistivity are discussed in the terms of possible f-electron *dualism* in UGe<sub>2</sub> and its connection with the occurrence of superconductivity under pressure in this compound.

**Key words** : f-electron magnetism, magnetoelectron resistivity, superconductivity

### 1. Introduction

The discovery of superconductivity (SC) under pressure in the ferromagnetic UGe<sub>2</sub> ( $T_C=53$  K and  $\mu_S \approx 1.4 \mu_B$  at ambient pressure) [1] was associated with the observation of a broad anomaly in the temperature derivative of the resistivity having a maximum at so called the characteristic temperature  $T^*$  ( $\approx 30$  K), first reported by Oomi [2].  $T^*$  was also clearly detected in the coefficient of volume thermal expansion  $\alpha_V$  [3]. This coefficient first decreases discontinuously at  $T_C$  and then slowly increases with cooling exhibiting a small dip feature at  $T^* \approx 25$  K, suggesting a somehow phase transition in the ferromagnetic phase. As a reason of some scattering in the observed  $T^*$  values, the authors of Ref. [3] have given the fact of using different single-crystalline samples in the electrical and thermal expansion measurements.

This temperature at ambient pressure is around 30 K and just reaches zero at the critical pressure  $p_C^* \approx 12$  kbar, where  $T_{SC}$  becomes the highest (0.8 K) [1]. At the same time,  $T_C = 32$  K and  $\mu_S = 1 \mu_B$ , and the ferromagnetism (FM) disappears at QCP, where critical pressure  $p_C \approx 16$  kbar. Until now the nature of the characteristic temperature  $T^*$  has been a matter of intensive debates in the literature. Most of the works devoting to the

coexistence of SC and FM in UGe<sub>2</sub> have been focused so far on the electronic and magnetic properties of this compound under pressure. It is natural to think, however, that the proceeding reason of the occurrence of SC in UGe<sub>2</sub> under pressure lies first of all in detailed recognizing these properties at ambient pressure.

Recently, we have discovered around  $T^*$  an unusual temperature dependence of the transverse magnetoresistivity (TMR), first on the poly- [4] and then on single-crystalline [5] UGe<sub>2</sub> samples. The TMR measured for a UGe<sub>2</sub> single crystal along the three main axes was found to be highly anisotropic. At low temperature the TMR for the a, b, and c axes is positive and its magnitudes at 4.2 K and 8 T are in the following proportions 1:4:2, respectively. It should be mentioned here that in the orthorhombic crystal structure of ZrGa<sub>2</sub>-type in which UGe<sub>2</sub> crystallizes, the lattice parameter b/a ratio is as large as 3.75. This clearly shows that the smallest effect is for the easy axis a and the largest one is for the most hard direction b. At temperatures above about 15 K (b-axis) and 25 K (a- and c-axis) the TMR becomes negative with a distinct minimum at  $T_C$ , as one would expect for a ferromagnet, but only for the latter two directions. However, the most spectacular behaviour is observed when the current  $j//b$  and the magnetic field  $B//a$ . Thus for this configuration the TMR goes through a very broad negative minimum where it achieves as high value as -40% at  $T=27$  K, i.e. at the temperature close to the

\*Corresponding author: Tel: (4871) 3435021, e-mail: troc@int.pan.wroc.pl

characteristic temperature  $T^*$ . Therefore, this effect in TMR can be considered as the most distinct and peculiar manifestation of the existing in UGe<sub>2</sub> of some kind of strong magnetic fluctuations taking place in the ferromagnetic order just at the temperature  $T_{sf} \approx T_C/2$  being close to  $T^*$ , but surprisingly without a trace manifestation at  $T_C$ .

In this work more detailed data are given on the magnetic and electrical properties of UGe<sub>2</sub> determined at ambient pressure on single-crystalline samples.

## 2. Experimental and Results

Two single crystals of UGe<sub>2</sub> denoted I and II were grown by a Czochralski method, as described earlier in Ref. 5. In this reference also the characterization of the sample I is given.

We synthesized also a polycrystalline sample of ThGe<sub>2</sub> by melting the components in an arc-furnace under argon atmosphere and followed annealing under vacuum at 800 °C for 4 weeks. X-ray examination revealed a single phase of the ZrSi<sub>2</sub>-type (s.g. Cmmm) with the lattice parameters:  $a = 1.6623(2)$ ,  $b = 0.4019(4)$  and  $c = 0.4144(4)$  nm. Any attempt to obtain the isostructural to UGe<sub>2</sub> phase of ThGe<sub>2</sub>, i.e. of the ZrGa<sub>2</sub> type (s.g. Cmcm) has failed. The latter phase was previously reported by Brown [6] in his crystal structure refinement of both types. Both these type structures, however, are closely related to each other and can be derived by a simple crystallographic translation.

The measurements of susceptibility, magnetization and electrical resistivity were made on both as-grown single crystals of UGe<sub>2</sub>. The magnetization measurements were carried out in magnetic fields up to 5 T in the temperature range 1.9–300 K using a SQUID magnetometer. The electrical resistivity measurements in zero (up to 300 K) and magnetic-fields up to 8 T (up to 90 K) were made by the dc-four probe method. The resistivity measurements of ThGe<sub>2</sub> were performed on a rectangular parallelepiped cut off from a bulk sample.

### 2.1. Magnetic susceptibility

Fig. 1 displays the temperature dependence of the reciprocal paramagnetic susceptibility for the field oriented along the a-, b- and c- axes. In accordance with previous such studies [7, 8], a large anisotropy in these dependencies is well apparent. Most probably that the observed anisotropy in the susceptibility behaviour, where  $\chi_a \gg \chi_c > \chi_b$ , is clear evidence that essentially the localized 5f electron states exist in UGe<sub>2</sub> and the crystal electric field (CEF) effects is mainly responsible for this

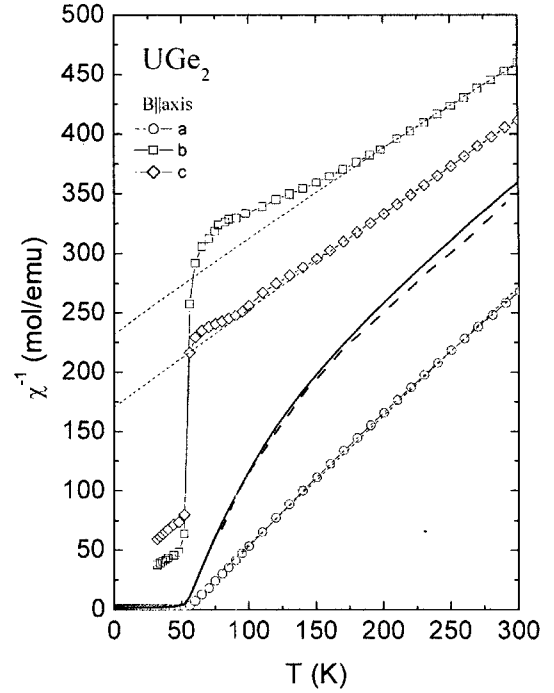


**Fig. 1.** Reverse molar magnetic susceptibility measured for magnetic field applied along three main crystallographic axes a, b and c. In addition the calculated curves:  $\chi_{av}^{-1}(T)$  (solid line) and  $\chi_{poly}^{-1}(T)$  (dashed line) taken from Ref. 7 are also given.

feature. The obtained magnetic characteristics by fitting the susceptibility to the modified Curie-Weiss law are presented in Table 1. There are both small and large differences compared with the previous not so precise data [7, 8] as those presented here. Menovsky *et al.* [7] found that the susceptibility measured in fields applied along the easy axis a ( $\chi_a$ ) is well defined by a Curie-Weiss law with  $\mu_{eff} = 2.67 \mu_B$  and  $\theta_{CW} = -53$  K, while Onuki *et al.* [8] on the basis of the Curie-Weiss law fitting to their susceptibility data, but above 200 K, have estimated the effective numbers of Bohr magnetons (and the paramagnetic Curie temperatures) to be  $3.0 \mu_B$  (0 K),  $3.2 \mu_B$  (-270 K) and  $3.1 \mu_B$  (-190 K), respectively. In Fig. 1 there are also shown the temperature variations of an average susceptibility,  $\chi_{av} = \chi_a + \chi_b + \chi_c/3$ , compared to the reported  $\chi_{poly}$  results [7], obtained on the polycrystalline sample. As seen, the  $\chi_{av}^{-1}(T)$  and  $\chi_{poly}^{-1}(T)$  curves coincide. No such a good agreement exists with respect to

**Table 1.** The MCW parameters for UGe<sub>2</sub> single crystal I

Axes	$\rho_0 (10^{-3} \text{ emu/mol})$	$T_p$ (K)	$\mu_{eff} (\mu_B)$
a	0.43	56	2.55
b	0.38	-254	2.83
c	0.15	-199	3.02

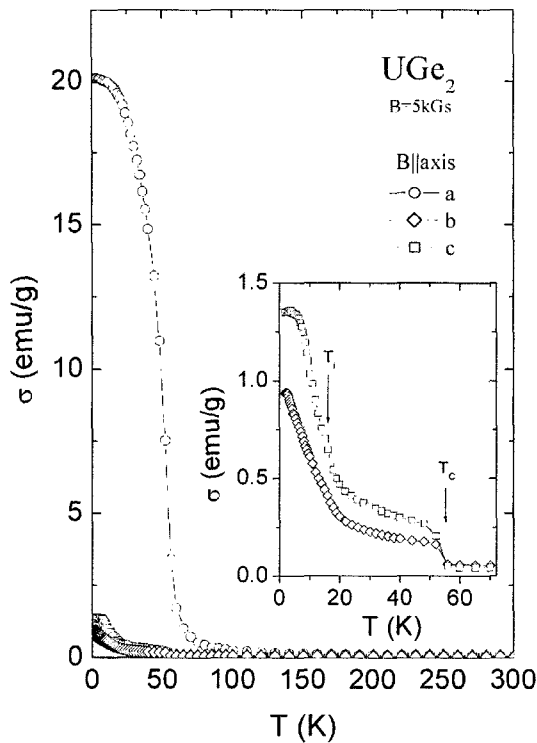


Fig. 2. Magnetization  $\sigma_a$  as a function of temperature. This function for  $\sigma_b$  and  $\sigma_c$  are shown in the inset.

the data of Ref. 8, probably caused by some preferential effect in grain orientation. It is clear that the strong curvature in  $\chi_{\text{poly}}^{-1}$  versus  $T$  arises just from the large anisotropy in the susceptibilities, measured along main crystallographic directions.

Considering the temperature variation of the reverse susceptibilities with fields applied along the b- and c-hard directions, one notes the upward deviations in  $\chi_i^{-1}(T)$  for both cases ( $i = c$  and  $b$ ) below about 200 K, which might signal the presence of the CEF splitting with singlets as the ground and excited states corresponding to the  $5f^2$  electronic configuration of the uranium atoms in  $\text{UGe}_2$ . Hence the FM in  $\text{UGe}_2$  and so huge anisotropy probably are of induced type [9].

In the  $\text{ZrGa}_2$ -type structure the central U atom is surrounded by the 8 nearest germanium atoms which form a slightly distorted antiprismatic  $\text{UGe}_8$  yielding strongly an axial CEF potential on the central magnetic atom just along the b-axis. As is well known, for the regular antiprismatic configuration having  $D_{4d}$  point symmetry around the  $\text{U}^{4+}$  ion ( $^3H_4$ -term) one would deal with four ion-Kramers doublets:  $|\pm 4\rangle$ ,  $|\pm 3\rangle$ ,  $|\pm 2\rangle$  and  $|\pm 1\rangle$  and one singlet  $|0\rangle$ . One of them may be a ground state depending on the  $c/a$  ratio (here the  $b/a$  ratio because  $a \parallel c$ ) and the remaining states form the excited states (see for example Ref. 10). The parametrization of the crystal field

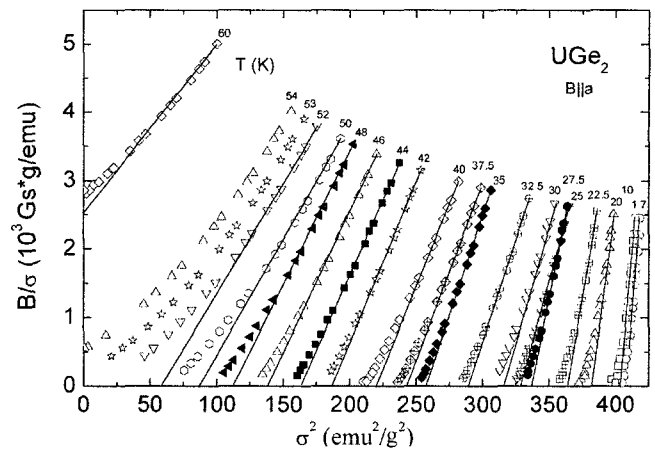
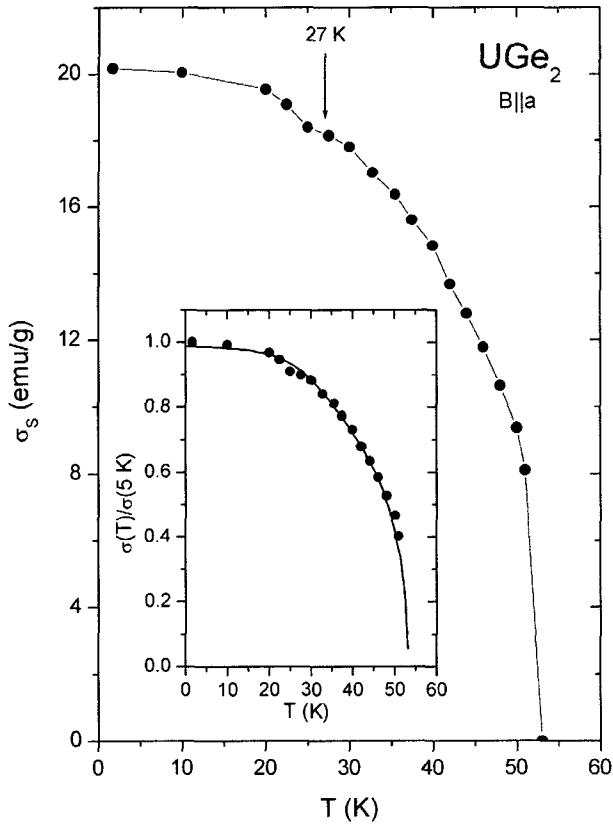


Fig. 3. The Arrot plot taken along the easy magnetization axis a.

potential and the splitting diagrams for the lower symmetries than  $D_{4d}$ , yielding only CEF singlets, where one of scheme could be adequate for the case of  $\text{UGe}_2$ , has been reported, e.g. in Ref. 11 in Fig. 3. Closer inspection of the antiprismatic indicates, that the distances: U-4Ge(1), U-2Ge(2) and U-2Ge(3) are close to one another and are as follows: 0.297, 0.295 and 0.292 nm, respectively. The two other distances U-2Ge(1) in the case of  $\text{UGe}_{10}$  configuration equaling to 0.323 nm, seem to be too large, and they should not be taken into account..

## 2.2. Magnetization

The magnetization curves measurement performed at 1.9 K along main crystallographic directions (not shown here) gave very similar results to those already reported in the literature [7, 8]. These measurements have confirmed that the direction of an easy magnetization is the shortest axis (a-axis) and that the value of the ferromagnetic moment along this axis is about  $1.4 \mu_B$ . The magnetization curves taken for this axis at temperatures between 1.7 and 80 K together with those showing temperature dependence of magnetization, measured in fields from 50 Gs to 10 kGs were presented elsewhere [5]. Here, there is demonstrated in Fig. 2 the thermal dependence of the magnetization taken at 5 kGs along three main crystallographic directions. This figure illustrates first of all the fact how small values of the magnetic moments are reached at 1.9 K for the b- and c-hard directions ( $0.07$  and  $0.096 \mu_B$ , respectively) in relation to the value of  $1.4 \mu_B$  found along the easy axis. Thus, this gives also a scale of huge anisotropy. In the inset of Fig. 2 the temperature variations of the magnetization along the hard b- and c-axes are shown. It appears, that these dependencies are not of a Brillouin curve type and differ in their shape from that measured along the easy axis, which is typical



**Fig. 4.** The extracted from the Arrot plot (Fig. 3) the spontaneous magnetization  $s_s$  as a function of temperature (solid circles). The inset shows for the reduced  $\sigma_s(T)/\sigma_s(5 \text{ K})$  magnetization (solid circles) compared to that determined in the neutron diffraction measurement, taken from Ref. 17 (solid line), both are plotted as a function of temperature.

for a ferromagnet. Namely, for the b- and c-axes the  $s$  versus  $T$  curves show an inflection point at about 15 K followed by a long tail up to  $T_C$ .

Magnetization data in a wide temperature range from 1.9 K to 60 K are presented in Fig. 3 in fashion of so called “Arrot plot”, i.e.  $\sigma^2$  versus  $B/\sigma$ . The extrapolation of high field  $B/s$  values to zero yields the square spontaneous magnetization  $\sigma_s^2$ . Then the  $\sigma_s$  values were inferred from the above extrapolation and have been plotted against the temperature in Fig. 4. Although it concerns practically the only one extracted point, a small depression in the vicinity of  $T^*$  is seen. Furthermore, their reduced values  $\sigma_s(T)/\sigma_s(0)$  are also compared in the inset of this figure to a similar curve obtained from the neutron diffraction data [1]. An agreement between these two experiments is quite good. However, it is interesting to note that such a simple extrapolation used at lower temperatures fails at higher temperatures to get  $T_C \approx 53 \text{ K}$  as expected. Earlier such a plot but for only several temperatures around  $T_C$  was presented by Menovsky *et al.*

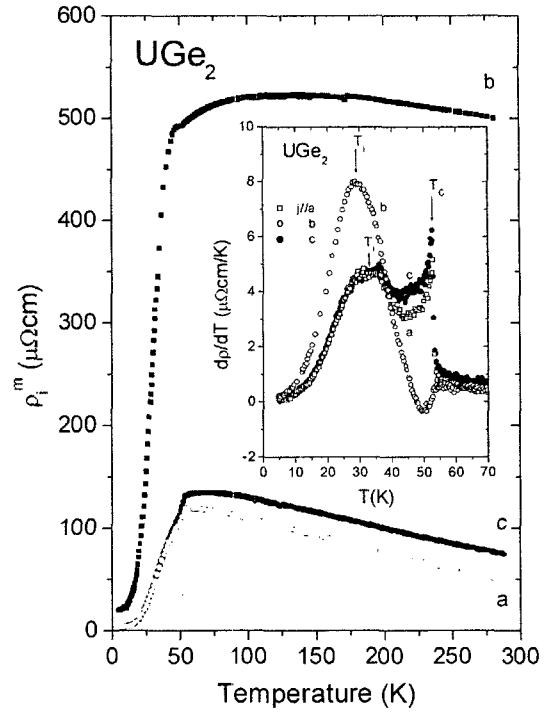


**Fig. 5.** Only the magnetic part of the resistivity  $\rho_i^m$ , where  $i = a, b$  and  $c$ , as a function of temperature measured for sample I. The inset shows the temperature derivative of the resistivity,  $d\rho(T)_i/dT$ , determined for sample II.

[7] which had a similar fashion with a strong curvature of the  $\sigma^2$  versus  $B/\sigma$  function for  $B/\sigma \rightarrow 0$ . In both situations a strong curvature of this function close to the transition temperature does not allow to determine precisely the Curie point by this method.

### 2.3. Electrical resistivity and magnetoresistivity

Electrical resistivity was measured on two oriented single crystals I and II, cut off from different batches. We have also measured  $\rho(T)$  for the polycrystalline sample of ThGe<sub>2</sub>, considering it as a diamagnetic reference for UGe<sub>2</sub>. The measured  $\rho(T)$  curve between 4.2 and 300 K for this compound is typically of metallic character, i.e. it shows a “hockey stick” shape. Fig. 5 demonstrates the extracted magnetic part of the UGe<sub>2</sub> resistivity  $\rho_i^m$  ( $i = a, b, c$ ) versus  $T$ , obtained for sample I by subtraction from the total  $\rho_i(T)$  the phonon part by using in this purpose the only temperature dependence of the reference resistivity of ThGe<sub>2</sub>. From this figure it is clear that along the hard directions, where  $j//b$  and  $j//c$ , the slope  $d\rho_i^m/dT$  becomes negative, which reminiscent a Kondo effect, while for the  $j//b$  configuration this is not so apparent. It appears that the  $\rho_b(T)$  curve above  $T_C$  goes through a wide maximum at 175 K. In this figure the temperature derivative of the resistivity found for three main axes is

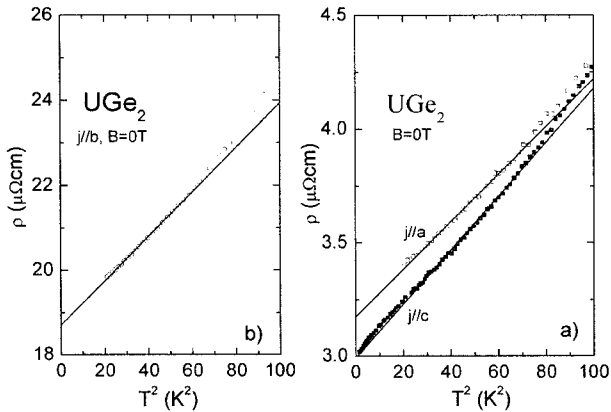


**Fig. 6.** The  $\rho_i$  vs  $T^2$  Fermi-liquid function determined for three main crystallographic directions.

also displayed in the inset. If  $T_C$  is exactly same for all three directions, the inflection point  $T_i$  determined by a maximum in  $d\rho(T)/dT$  for the b-axis is found at lower temperature than that for the a and c-axes. It has been discussed in Ref. 4 that  $T_i$  corresponds to the characteristic temperature  $T^*$ .

As shown in Fig. 6, the electrical resistivity measured along the three main crystallographic directions can be fitted below about 8 K to the expression:  $\rho_i(T) = \rho_{i0}(T) + A_i T^2$  ( $i = a, b, c$ ), following of which may indicate the presence of both the magnetic fluctuations (Fermi-liquid state) and/or spin wave excitations. The latter due to the Ising type of the magnetization [12] somehow precludes the latter contribution. The obtained parameters are presented in Table 2. Previously the values of the coefficient  $A_i$  were given only for  $\rho_a$  ( $j//a$ ) [2], for  $\rho_{poly}$  [13] and for  $\rho_x$  (not defined direction) [14, 15]. All these reported data are close to those given in Table 2 for the a- and c-axes. As this Table indicates, the  $A_b$  value is almost 5 times larger than those of  $A_a$  and  $A_c$ . This kind of anisotropy in the  $A_i$  coefficients should be explained in the future studies. As is known, the magnitude of the coefficient  $A$  is connected with the strength of magnetic fluctuations and with a magnitude of  $T_{sf}$  ( $A \sim T_{sf}^{-2}$ ). For further discussion see also Ref. 4.

In Fig. 7 we have plotted the magnetoresistivity  $\Delta\rho/\rho_0$ , defined as the ratio  $[\rho(T,B) - \rho(T,0)]/\rho(T,0)$ , against

**Table 2.** Fermi-liquid characteristics of a  $UGe_2$  single crystal (sample I)

$\rho_i$	$\rho_0$ ( $\mu\Omega\text{cm}$ )	$A_i$ ( $\mu\Omega\text{cm}/\text{K}^2$ )
a	3.2	0.011
b	18.7	0.052
c	3.03	0.012

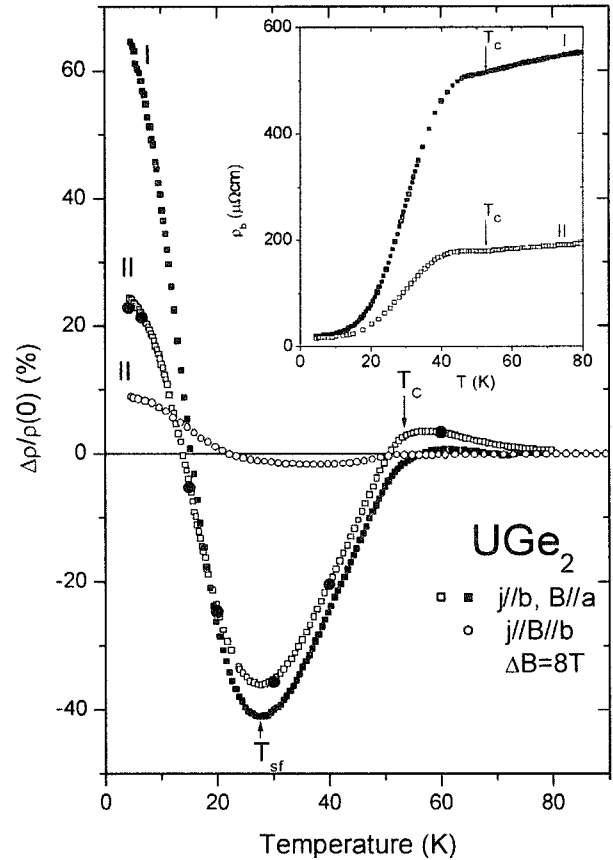


**Fig. 7.** Transverse (for samples I and II, solid and open squares, respectively) and Longitudinal (sample II, open circles) magnetoresistivity,  $\Delta\rho/\rho(0)$  vs.  $T$ , measured for the current  $j$  flowing along the b-axis and at 8 T applied perpendicular to the current direction. The large solid circles are the data taken from the  $\Delta\rho/\rho(0)$  vs  $B$  curves at 8 T for sample II (not shown here). The inset shows the different temperature behaviour of  $\rho_b$  for samples I and II.

temperature for both single crystals measured. Practically the difference between samples I and II exists only at low temperatures. This results together with those earlier published in Ref. 5 for sample I clearly indicate the presence of huge effect in  $D\rho/\rho_0(T)$  at  $T_{sf}$  near the characteristic temperature  $T^*$  of  $UGe_2$ . In the inset to this figure the  $\rho_b(T)$  curves measured for samples I and II are presented. Although there were only negligible differences in the lattice parameters between the samples [see for the values in Ref. 5], the electrical resistivity measured for the current  $j//b$  showed  $\rho_b$  (300 K) almost to be three times larger for sample I compared to that for sample II, but with almost the same value of  $\rho_0 \approx 20$  mWcm for both the samples. Despite the higher value of RRR for the former sample (31.5 against 14.0) a quite good agreement with the  $\rho(T)$  data of Onuki *et al.* [8] was just found for sample II with lower RRR value. It should

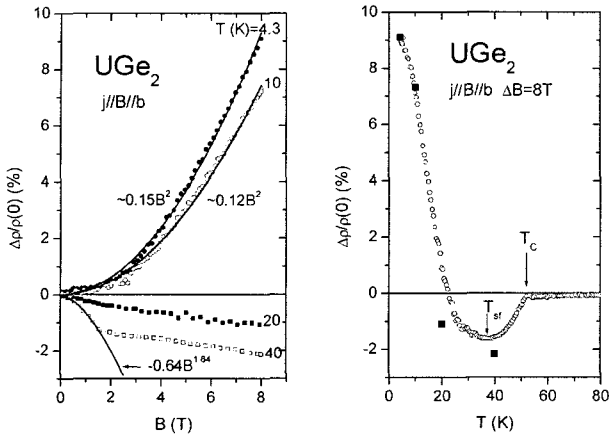


**Fig. 8.** The longitudinal magnetoresistivity (LMR) measured at various temperatures as a function of applied field  $B$  up to 8 T (left hand panel) and measured at 8 T as a function of temperature  $T$  up to 80 K (right hand panel).

be mentioned that the RRR values of the single crystals reported in Ref. 8 are about an order of magnitude higher than those presented here indicating a very good quality of samples used. Nevertheless, the character of  $\rho(T)$  and the Fermi-liquid parameters are practically the same for both measurements. In accordance to the data of Onuki *et al.* [8] there is well seen a hump in this dependences just below  $T_C$ , as marked by the arrows in the inset of Fig. 7. The origin of the hump, observed only for the  $j//b$  configuration, is still not explained. This would be so far the only eventual signal of the existence of a spin density wave (SDW) behaviour in UGe<sub>2</sub>, but detected only along the expanded  $b$  axis. The latter has been predicted theoretically [16] to occur at temperatures below  $T^*$ , but still not being confirmed experimentally by neutron scattering methods [1, 17].

Finally in Fig. 8 there is demonstrated for the first time the field (figure a) and temperature (figure b) dependencies of  $\Delta\rho/\rho(0)$ , measured for sample II but in the configuration  $j//b//B$ , yielding the longitudinal magnetoresistivity (LMR) along the magnetization hard direction  $b$ . It becomes clear in Fig. 6 that the effect is considerably smaller in comparison to that found in TMR, especially at the temperature range where the MR becomes negative. As is seen in Fig. 7a, the field dependences of at temperatures 20 and 40 K are almost linear in  $B$ , while at lower temperatures it changes as a  $B^2$ . Interestingly, as shown in figure (b), the temperature dependence of  $\Delta\rho/\rho(0)$  exhibits a similar character as that of TMR, but the LMR value at the negative maximum, occurring also near  $T^*$ , is only 5% of that observed at  $T_{sf}$  of TMR. For LMR, the latter temperature seems to be shifted a little to higher temperatures, compared to that of TMR. Again, no effect

in LMR is seen at  $T_C$ . The difference in LMR and TMR is shown in Fig. 6. It probably arises from a large anisotropy existing in the magnetic fluctuations depending on the mutual configuration of the current and field, being further in the relation to the crystallographic axes.

### 3. Discussion

The properties which have been revealed under pressure in UGe<sub>2</sub>, where the relatively strong and highly anisotropic FM allows or may even induce SC, can not be understood in terms of existing theories and need a novel concept [18]. A new mechanism of simultaneous appearance of ferromagnetism and superconductivity based on interaction of electrons mediated by localized moments has recently been proposed by Suhl [19] and Abrikosov [20]. In their model the simultaneous onset of magnetic order and superconductivity may be explained as a coupling of two conduction electrons *via* one localized moment. Here, especially on the basis of recently performed studies aimed at the determination of the Fermi surface (FS) in the paramagnetic state of UGe<sub>2</sub> [21], it becomes clear that FM comes from the fairly well localized  $5f^{3-n}$  electrons, with  $n \approx 1$ , while Cooper pairs probably originate from medium heavy quasiparticles (the electronic heat capacity coefficient  $\chi(0) = 30$  mJ/K<sup>2</sup>mol [22]) formed by the hybridized  $5f^n$  electrons with the conduction electrons, which microscopically emphasizes the double role of the  $5f$  electrons in this compound. In the circumstances of existing a large internal field due to FM, the only so called nonunitary triplet state, being free from the Pauli limit, can be taken into account as the SC-state [23]. Thus spin (magnetic) fluctuations as a mediated pairing mechanism in the case of such a state has been proposed which seems to be in line with the discovery in Ref. 5 of the huge magnetoresistivity effect detected deeply in the ferromagnetic state and being confirmed here by carrying out the MR measurements on the different single-crystalline samples of UGe<sub>2</sub>. The decrease of the resistivity by about 40% at the temperature close to  $T^*$  could only be possible by depressing magnetic fluctuations by an applying a field of 8 T along the easy axis  $a$  with the current flowing along the most hard and largely elongated  $b$ -axis. Furthermore, the more detailed studied under pressure of the coefficient  $A_b$  in the Fermi-liquid formula just along the  $b$ -axis in the vicinity of  $p_C^*$  can probably give more arguments about the role of the magnetic fluctuations, detected along the  $b$ -axis, in the creation of SC in UGe<sub>2</sub>. As we have signaled above this coefficient at ambient pressure is about 5 times larger than the remaining  $A_a$  and  $A_c$  coefficients. If only a

modulation of FM by SDW will be detected in the future, one then can think that the fluctuations of coupled charge density- (CDW) and spin density-(SDW) waves, postulated in the literature [16], are just those which are responsible for the MR effect, described in this work. Very recently a microscopic model for ferromagnetism of  $UGe_2$ , which takes into account the competition of the orbital degeneracy of the 5f electrons as well as the anisotropies of the CEF and hopping terms has been proposed [24]. In consequence one of possible magnetic moment arrangements is the transverse to the (ac)-plane a SDW component but with a small magnetic amplitude of  $0.01 \mu_B$ , the value considerably lower than the resolution of neutron scattering experiment [17], but in accordance with results of positive muon spin relaxation measurements performed on a  $UGe_2$  single crystal [25]. In the latter work in addition to the well-known localized 5f-electron density responsible for the ferromagnetic bulk properties, the existence of itinerant quasistatic magnetic correlation with magnetic moment of about  $0.02 \mu_B$  has been found. All these findings seems to be supported by the recently observed electronic-kind transition near  $T^*$  in the Hall effect experiment performed on a single crystal of  $UGe_2$  [26].

### Acknowledgment

The author is grateful to Professor Takemi Komatsubara for his kind help during preparation of the  $UGe_2$  single crystals and to R. Gorzelniak and D. Badurski for their assistance in the measurements. The work was supported by KBN Grant No.2 PO3B 109 24.

### References

- [1] See a vast Review: A. Huxley, I. Sheikin, E. Ressouche, N. Kernavanois, D. Braithwaite, R. Calemczuk, and J. Flouquet, *Phys. Rev. B* **63**, 1444519 (2001) and references therein.
- [2] G. Oomi, Y. Kagayama, and Y. Onuki, *J. Alloys Comp.* **271-273**, 482 (1998).
- [3] G. Oomi, M. Ohashi, K. Nishimura, and Y. Onuki, *J. Nucl. Sc. Techn., Suppl.* **3**, 90-93 (2002).
- [4] R. Troc, H. Noël, and P. Boulet, *Phil. Mag. B* **82**, 805 (2002).
- [5] R. Troc, *Acta Phys. Polon. B* **34**, 407 (2003).
- [6] A. Brown, *Acta Cryst.* **15** (1962) 652.
- [7] A. Menovsky, F. R. de Boer, P. H. Frings, and J. J. M. France, in *High Field Magnetism*, ed. M. Date (North-Holland Publishing Company, 1983) p. 189.
- [8] Y. Onuki, I. Ukon, S. W. Yun, I. Umehara, K. Satoh, T. Fukuhara, H. Sato, S. Takayanagi, M. Shikama, and A. Ochiai, *J. Phys. Soc. Japan* **61**, 293 (1992).
- [9] J. J. M. Franse, P. H. Frings, F. R. de Boer, and A. Menovsky, in *Physics of Solids under High Pressure*, R. N. Shelton (ed.), North-Holland Publ. Co. (1981) p. 181.
- [10] J. Mulak, and A. Czopnik, *Bull. Acad. Polon. Sci., Ser. Sci. Chim.* **20**, 209 (1972).
- [11] Z. Gajek, J. Mulak, and J. C. Krupa, *J. Sol. St. Chem.* **107**, 413 (1993).
- [12] S. Raymond, and A. Huxley, *Physica B* **350**, 33 (2004).
- [13] E. D. Bauer, R. P. Dickey, V. S. Zapf, and M. B. Maple, *J. Phys.: Condense Matter* **13**, L759 (2001).
- [14] N. Tateiwa, T. C. Kobayashii, K. Hanazono, K. Amaya, Y. Hagle, R. Settai, and Y. Onuki, *J. Phys.: Condense Matter* **13**, L17 (2001).
- [15] T. C. Kobayashi, K. Hanezono, N. Tateiwa, K. Amaya, Y. Haga, R. Settai, and Y. Onuki, *J. Phys.: Condense Matter* **14**, 10779 (2002).
- [16] S. Watanabe, and K. Miyake, *J. Phys. Soc. Japn.* **71**, 2489 (2002).
- [17] N. Kernavanois, B. Grenier, A. huxley, E. Ressousche, J. P. Sanchez, and J. Flouquet, *Phys. Rev. B* **64**, 174509 (2001).
- [18] K. Machida, and T. Ohmi, *Phys. Rev. Lett.* **86**, 850 (2001).
- [19] H. Suhl, *Phys. Rev. Lett.* **87**, 167007 (2001).
- [20] A. A. Abricosov, *J. Phys.: Condens. Matter* **13**, L943 (2001).
- [21] M. Biasini, and R. Troc, *Phys. Rev. B* **68**, 245118 (2003).
- [22] S. W. Yun, K. Satoh, Y. Fujimaki, I. Umehara, Y. Onuki, S. Takayanagi, H. Aoki, S. Uji, and T. Shimizu, *Physica B* **186-188**, 129 (1993).
- [23] T. Ohmi, and K. Machida, *Phys. Rev. Lett.* **71**, 625 (1993).
- [24] K. Hirohashi, and K. Ueda, *J. Phys. Soc. Jap.* **73**, 1576 (2004).
- [25] A. Yaouanc, P. Dalmas de Réotier, P. C. M. Gubbens, C. T. Kaiser, A. A. Menovsky, M. Mihalik, and S. P. Cottrell, *Phys. Rev. Letters* **89**, 147001 (2002).
- [26] V. H. Tran, S. Pachen, R. Troc, M. Baenitz, and F. Steglich, *Phys. Rev. B* **69** (2004) 195314.